Formation of color centers in a soda-lime silicate glass by excimer laser irradiation

2010 J. Phys.: Condens. Matter 22 045901

(http://iopscience.iop.org/0953-8984/22/4/045901)

J. Phys.: Condens. Matter **22** (2010) 045901 (7pp) doi:10.1088/0953-8984/22/4/045901

Formation of color centers in a soda-lime silicate glass by excimer laser irradiation

Kohei Kadono[1,5], Nobuyuki Itakura[2], Tomoko Akai[3], Masaru Yamashita[3] and Tetsuo Yazawa[4]

[1] Division of Chemistry and Materials Technology, Kyoto Institute of Technology, Matsugasaki, Sakyo-ku, Kyoto 606-8585, Japan
[2] Glass Research Center, Central Glass Co., Ltd, 1510 Ohkuchi-cho, Matsusaka, Mie 515-0001, Japan
[3] National Institute of Advanced Industrial Science and Technology (AIST), Midorigaoka, Ikeda, Osaka 563-8577, Japan
[4] Graduate School of Engineering, University of Hyogo, Shosha, Himeji, Hyogo 671-2201, Japan

E-mail: kadono@kit.ac.jp

Received 25 August 2009, in final form 30 October 2009
Published 5 January 2010
Online at stacks.iop.org/JPhysCM/22/045901

Abstract
We have investigated defect generation in soda-lime silicate and iron-doped soda-lime silicate glasses by excimer laser irradiation in order to apply coloration due to radiation-induced defects as a coloring technique for practical glass products. The laser irradiation generated various kinds of defects, i.e., non-bridging oxygen hole centers (NBOHCs), E′ centers, and trapped electron centers, as does x-ray and γ-ray irradiation. The amounts of generated NBOHCs, monitored by the absorption intensity, increased at first with the irradiation time for both the ArF and XeF lasers, and eventually became saturated. The saturated values for the ArF laser irradiation were almost the same regardless of the laser intensity, whereas those for the XeF laser irradiation were dependent on the intensity; a higher intensity generated a larger amount of NBOHCs. From the comparison of the energies of the photon and the absorption edge of the soda-lime silicate glasses, the defect generation reactions were expected to be one-photon and two-photon processes for the ArF and XeF lasers, respectively. In order to explain the defect generation behavior, we used a simple kinetic model in which the NBOHCs are reversibly generated and annihilated through the photo-reaction. The model includes a stretched exponential function, which is often observed for reactions occurring in amorphous materials. The dependences of the amounts of the generated NBOHCs on the irradiation time and intensity of the laser pulses derived from the model were consistent with the experimental results.

(Some figures in this article are in colour only in the electronic version)

1. Introduction

It is well known that high energy irradiation of glasses induces various kinds of defects [1–7]. When the glasses are based on multi-component systems consisting of alkali and alkaline earth oxides, one of the representative defects is the non-bridging oxygen hole center (NBOHC) [1–5]. NBOHCs in multi-component glasses have strong absorption in the visible region and make the glasses a brownish color. Since the color resembles the amber color, which is commonly used for colored glass containers, we have proposed that the coloration induced by the high energy irradiation of glasses be applied for practical glass products [8–13]. The advantage compared with the conventional coloration of glasses, in which transition metal ions or colloidal particles are incorporated into glasses, is that irradiation-induced colors can easily be bleached by heat treatment. Thus, glasses colored by irradiation can be recycled as if they were colorless glasses and without any separation processes being required between colored and colorless glasses [8].

[5] Author to whom any correspondence should be addressed.

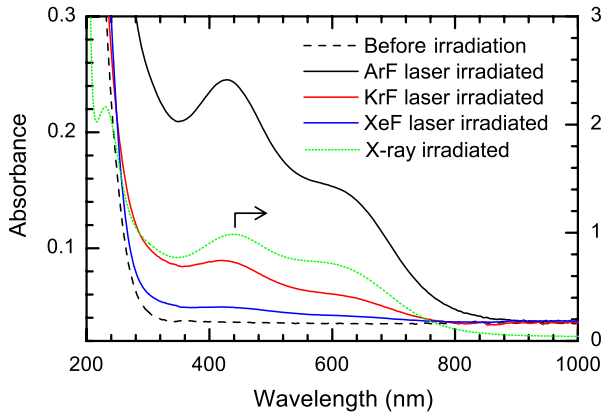

Figure 1. Absorption spectra of the base glass (broken line) and those irradiated by the ArF, KrF, and XeF lasers (solid lines) and x-rays (dotted line). The irradiation conditions for the lasers were 78 mJ cm^{-2} in intensity operated with a repetition rate of 10 Hz for 1 h. The x-ray irradiation time was 10 min.

The high energy radiation generally used for the defect generation is x-rays and γ-rays. On the other hand, well developed UV lasers, such as excimer lasers, also generate defects in glasses. The defects, and their generation and annihilation by excimer laser irradiation have been investigated for various kinds of silica glasses [6, 7, 14–21] and other glasses used for the UV region, such as phosphate and fluorophosphates glasses [22–28]. However, there are few studies on the soda-lime silicate glasses used for the conventional glass products. If UV laser irradiation can be used for the brownish coloration of soda-lime silicate glasses, we expect that the technique would have highly potential applications because of the possibility for drawing lines and pictures.

In the present study, we investigated the behaviors of the generation and annihilation of irradiation-induced defects, particularly, focused on NBOHCs in soda-lime silicate glasses using excimer lasers.

2. Experimental procedures

Glasses having the composition, $74SiO_2{\cdot}16Na_2O{\cdot}10CaO$ (mol%), were prepared from batch mixtures of reagent grade raw materials, SiO_2, Na_2CO_3, and $CaCO_3$. Glasses doped with 0.07 wt% of Fe_2O_3 (for 100 wt% of the undoped glass) were also prepared in order to investigate the effects of iron on the radiation behavior. The concentration of the iron was decided as a typical content of the impurity iron in sheet glasses. The batches were melted in Pt crucibles at 1400 °C for 3 h under air atmosphere and were cast into carbon molds. The glasses were annealed at 500 °C. The obtained glasses were cut into 2 mm thickness and both sides were optically polished. The undoped and Fe_2O_3-doped glasses are referred to as base and Fe-doped glasses, respectively. Ultraviolet laser irradiation was performed using three kinds of excimer laser, ArF (193 nm), KrF (248 nm), and XeF (351 nm), under various intensities and radiation times. The pulse durations of all the lasers were around 20–30 ns. The repetition frequencies were 1 or 10 Hz. X-ray irradiation was also performed for comparison, using an x-ray source of a Mo target ($\lambda = 0.7107$ Å at Kα line) operating at 50 kV and 50 mA.

Absorption spectra were measured with a spectrophotometer, Hitachi U-4100. Electron spin resonance spectra were obtained with a Bruker ESP 300E using a conventional X-band spectrometer at liquid N_2 temperature. The spectra were obtained at a power of 0.1 mW, a modulation amplitude of 0.1 mT, and a frequency of 100 kHz. The g values were calibrated using a diphenylpicrylhydrazyl (DPPH) standard with $g = 2.0036$.

In order to estimate experimental errors, we measured the irradiation time dependences of the absorption intensities several times under the same condition, i.e., about 76 mJ cm^{-2} ArF laser intensity and 10 Hz repetition with the use of the base glass (see section 3.2 in detail). The scatter of the absorbance data was within ±6 to ±9% for each irradiation time and ±8% in average.

3. Results and discussion

3.1. Generation of defects by excimer laser irradiation

Figure 1 shows absorption spectra of the base glasses which were irradiated with the excimer lasers and the x-ray together with that before irradiation. The irradiation conditions for all the lasers are 78 mJ cm^{-2} in intensity, operated with a 10 Hz repetition rate for 1 h. The irradiation time for x-rays was 10 min. For all the laser irradiated glasses, absorption bands with peaks at 430 and 620 nm were observed as well as the x-ray irradiated glass, although the absorption bands for the XeF laser irradiated glass were very weak. These absorption bands are assigned to the NBOHCs, HC_1 (430 nm) and HC_2 (620 nm), respectively [4, 5]. The glass irradiated by the ArF laser became brownish colored. In figure 2, the absorption spectra of the Fe-doped glass before and after ArF laser irradiation are shown with those of the base glass for comparison. The spectrum of the Fe-doped glass before irradiation showed a broad absorption at 800–1000 nm, which is assigned to the six-fold coordinated Fe^{2+} [29–31]. The small peak near the absorption edge is considered to be assigned to the absorption relevant to Fe^{3+} [29–32]. The red shift in the absorption edge is due to the charge transfer absorption between the iron and oxide ions [29–32]. The spectrum of the irradiated Fe-doped glass showed the same absorption bands as those of the irradiated base glass in the visible region, although the intensities were a little weaker. Figure 3 and table 1 show the peak decomposition results in which the subtraction spectra between those after and before the irradiation were decomposed into four Gaussian lines for the ArF laser irradiated and x-ray irradiated base glasses. In addition to the absorption bands at 430 nm (2.84 or 2.74 eV) and 620 nm (1.97 or 1.98 eV), 4.02 or 4.07 eV and 5.57 or 5.37 eV peaks were observed. These were assigned to the trapped electrons and E′ centers, respectively [3].

The ESR spectra around 345 mT of the ArF, KrF, and XeF laser irradiated base and ArF laser irradiated Fe-doped glasses are shown in figure 4. The spectrum of the x-ray

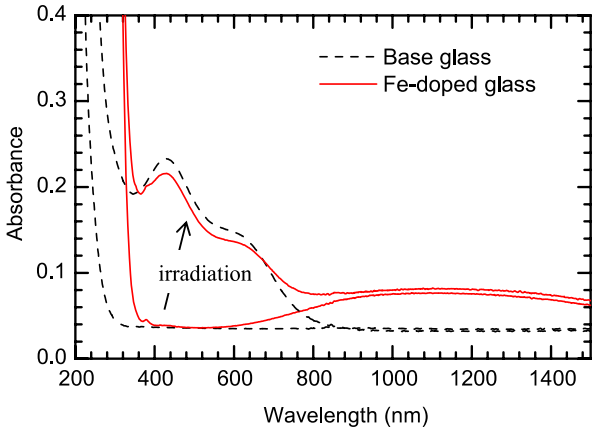

Figure 2. Absorption spectra of the base and Fe-doped glasses before and after the ArF laser irradiation. The irradiation conditions were the same as those in figure 1.

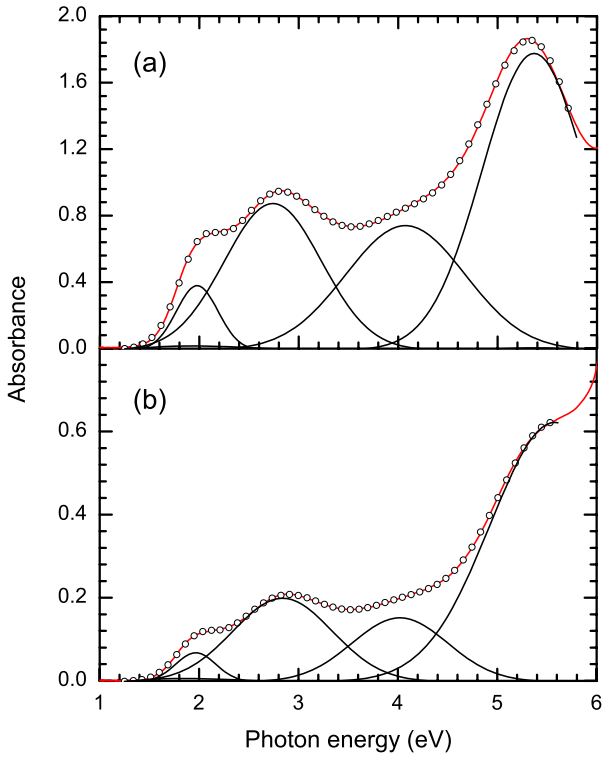

Figure 3. Peak decompositions for the subtraction spectra (red solid lines) between those after and before irradiation by (a) x-rays and (b) ArF laser. The summation of the four Gaussian lines are illustrated by circles.

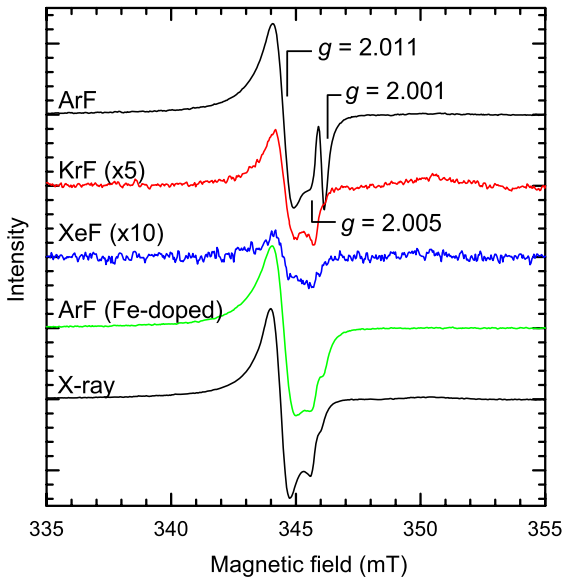

Figure 4. ESR spectra for the ArF, KrF, and XeF laser irradiated base glasses and the ArF laser irradiated Fe-doped glass, and the x-ray irradiated base glass.

Table 1. Results of the peak decomposition of the subtraction spectra between those after and before ArF laser and x-ray irradiation (see figure 3).

Assignment		ArF laser	X-ray
NBOHC (HC_2)	Peak position (eV)	1.97	1.98
	FWHM (eV)	0.48	0.49
	Peak height	0.070	0.39
	Relative peak area[a]	1.0	1.0
NBOHC (HC_1)	Peak position (eV)	2.84	2.74
	FWHM (eV)	1.18	1.15
	Peak height	0.20	0.88
	Relative peak area	7.1	5.3
Trapped electron	Peak position (eV)	4.02	4.07
	FWHM (eV)	1.13	1.42
	Peak height	0.15	0.75
	Relative peak area	5.2	5.6
E′ center	Peak position (eV)	5.57	5.37
	FWHM (eV)	1.53	1.23
	Peak height	0.62	1.79
	Relative peak area	29	12

[a] The peak area normalized to that of the absorption due to HC_2.

irradiated base glass is also shown for comparison. The signals at $g = 2.011$, 2.005, and 2.001 were assigned to the NBOHCs (HC_1 and HC_2) and E′ center, respectively [1–3, 7]. Comparing these with the spectra of the x-ray irradiated glass, it is a remarkable feature that the signal of the E′ center in the ArF laser irradiated base glass was strong. This was also indicated in the peak decomposition data of the absorption spectra in table 1, in which the relative intensity of the E′ center for the ArF laser irradiated base glass is 2.5 times larger than that of the x-ray irradiated one. This is probably due to the ArF laser irradiation promoting a generation reaction of the E′ centers such as

$$\equiv\mathrm{Si} - \mathrm{O} - \mathrm{Si}\equiv \rightarrow \equiv\mathrm{Si}\cdot + \cdot\,\mathrm{O} - \mathrm{Si}\equiv.$$

Here the bonding electrons between Si–O are more effectively excited by the photon energy of the laser resulting in the cleavage of bonds. The importance of this kind of reaction in silica glasses under irradiation by a F_2 laser was pointed out for E′ center generation, although the quantum yield was very low [16]. Although the yield is expected to further drop because of the relaxation of strained Si–O–Si bonds in the multi-component glasses, the reaction can occur

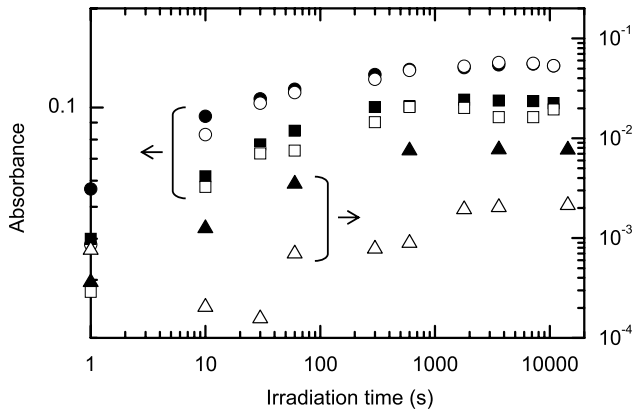

Figure 5. Irradiation time dependences of the absorption intensities at 620 nm for the base glasses irradiated by the ArF laser at 247 mJ cm^{-2} (●) and 76 mJ cm^{-2} (○), by the XeF laser at 263 mJ cm^{-2} (▲) and 65 mJ cm^{-2} (△), and the Fe-doped glass irradiated by the ArF laser at 247 mJ cm^{-2} (■) and 76 mJ cm^{-2} (□). The repetition frequencies were 10 Hz.

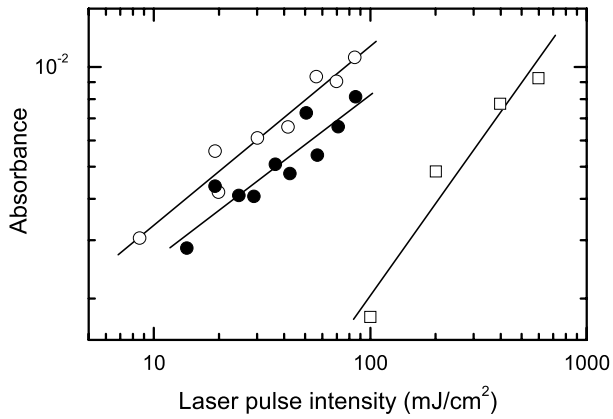

Figure 6. Dependences of the absorption intensities at 620 nm for the base glass on the laser pulse intensities by the ArF (○) and XeF (□) lasers and for the Fe-doped glass (●) by the ArF laser. The absorption intensities were measured after one and 1000 shots for the ArF and XeF lasers, respectively.

more efficiently under ArF laser irradiation than with x-ray irradiation.

3.2. Dependences of the defect generation on the irradiation time and intensities

Figure 5 shows the irradiation time dependences of the absorption intensities at 620 nm for the base glasses irradiated by the ArF and XeF lasers and the Fe-doped glass irradiated by the ArF laser. The irradiation was carried out for two different laser intensities, one was high intensity, 247 mJ cm^{-2} and 263 mJ cm^{-2} for the ArF and XeF lasers, respectively, and the other was low, 76 and 65 mJ cm^{-2}. Both repetition frequencies were 10 Hz. The absorption intensities increased with the irradiation time for all the experiments and reached saturated values at about 1000 s irradiation (10^4 shots). The saturated intensities of the induced absorption for both the base and Fe-doped glasses irradiated by the ArF laser were almost the same regardless of the pulse intensity. For the XeF laser irradiation, on the other hand, the saturated absorption induced by the high pulse intensity was higher than that by the low pulse intensity.

The dependences of the induced absorption intensities on the laser pulse intensities are illustrated in figure 6. The changes in absorption intensities after one shot irradiation for the ArF laser and after 1000 shots irradiation for the XeF laser operated at 10 Hz repetition frequency (after 100 s irradiation) are shown. The slopes were 0.54 and 0.49 for the base and the Fe-doped glasses by the ArF laser irradiation while it was 0.91 for the base glass by the XeF laser irradiation.

3.3. A kinetic model for the generation and annihilation of the defects

3.3.1. Formulation of the kinetic model based on the reversible generation and annihilation reaction. Various kinetic models have been proposed for the generation and annihilation of the defects induced by high energy radiation in silica [16, 18, 20, 33–35] and other glasses [22–26]. For instance, Mashkov *et al* obtained theoretical growth curves very consistent with experimental ones with a model which includes an irreversible generation reaction of the E′ centers from the glass network and a reversible reaction between the defects and the precursors [34]. Griscom reported that second-order kinetics could be applied for the generation and annihilation of the electron–hole pair defects [33, 35]. For both the theoretical treatments, 'stretched terms' were introduced in order to describe the distribution in the reaction processes. Imai *et al* [6, 7] and Kajihara *et al* [20, 21] proposed more concrete reaction models for the generation and annihilation of the E′ centers and NBOHCs in silica glasses irradiated by excimer lasers. For the defect generation induced by excimer laser radiation in multi-component glasses, Natura *et al* proposed kinetic models in which impurities in the glasses play an important role as an absorber and transferor of the photon energy for the defect generation [26]. They successfully obtained time evolution curves of the absorption intensity of the defects very consistent with the experiments.

Here we consider a simple kinetic model to explain the characteristic behaviors of defect generation by laser irradiation. This model is based on the reversible reaction of some structure units, s, which can be transformed to defects (NBOHCs), d, by the laser irradiation,

$$s \underset{k_r}{\overset{k_f}{\rightleftharpoons}} d.$$

Here, k_f and k_r present the rate constants for the defect generation and annihilation reactions. The forward reaction is activated by photons, while the reverse one may be not only photo-activated but also thermally activated. The number density of the s and d are represented by N_s and N, respectively, and

$$\frac{\mathrm{d}N}{\mathrm{d}t} = k_f N_s - k_r N. \tag{1}$$

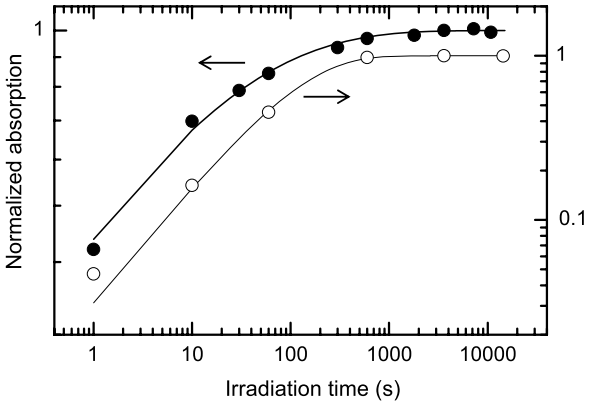

Figure 7. Curve-fitting results for the growth of the normalized absorption at 620 nm versus irradiation time for ArF laser (●) and XeF laser (○) irradiated base glass.

Assuming that $N_s \gg N$, N_s is almost constant and referred to as N_0. Then, equation (1) is solved as

$$N = \frac{k_f}{k_r} N_0 \left(1 - \exp(-k_r t)\right). \tag{2}$$

Here, in order to describe the distribution of the rate constants due to the distribution of the activation processes which are generally observed in amorphous materials [36, 37], the variable is changed by the next equation,

$$k_r t \rightarrow (k_r t)^{\beta}, \tag{3}$$

where $0 < \beta < 1$ [33–35]. Then we obtain a stretched exponential type of equation for the time dependence of the number of NBOHCs under irradiation,

$$N = \frac{k_f}{k_r} N_0 \left(1 - \exp(-(k_r t)^{\beta})\right). \tag{4}$$

Here, we briefly mention the most important structure unit represented by s, which is non-bridging oxygen (NBO). In this case, the defect generation and annihilation reaction can be written as

$$\equiv \mathrm{Si} - \mathrm{O}^- \rightleftarrows \equiv \mathrm{Si} - \mathrm{O} \cdot + \mathrm{e}^-.$$

The released electrons from the NBOs are trapped at various sites in the glasses, e.g., glass-modifying (alkaline and alkaline earth) ions and dopant cations (Fe^{3+} in our case). The reverse reaction is that the trapped electrons return to the NBOHCs through photo- or thermally activated processes. The potential energies of the trapped electrons, therefore, the activation energies for the reverse reaction, may vary from site to site resulting in the stretched exponential function expressed by equations (3) and (4). Protons can also trap the electrons and become hydrogen atoms, which may rapidly migrate in the glasses and bond to another hydrogen atoms, resulting in hydrogen molecules [5, 16, 18, 20]. In this case, the reverse reaction is diffusion controlled and thermally activated.

In the next two sections, we discuss the behaviors of the defect generation and annihilation by the use of equation (4).

Table 2. Fitting parameters using equation (4) for the experimental results shown in figure 5.

	Irradiation condition			
Glass	Laser	Intensity (mJ cm^{-2})	k_r (s^{-1})	β
Base	ArF	76	0.071	0.36
		247	0.148	0.29
	XeF	65	1.2×10^{-3}	0.57
		263	8.7×10^{-3}	0.72
Fe-doped	ArF	76	0.057	0.36
		247	0.085	0.32

3.3.2. Irradiation time dependence. The dependences of the defect generation on the irradiation time or the shot number for laser irradiation have been reported for silica glasses [6, 7, 15, 33–35], and phosphate and fluorophosphate glasses used in the UV region [22–27]. For all the cases, the number of induced defects increases with the irradiation time at first and then saturates. In the current experiments, a similar time or shot number dependence of the absorption intensities due to the NBOHCs was observed for both ArF and XeF laser irradiation. These time evolution curves were fitted using equation (4). The curve fittings are shown in figure 7 for the cases of ArF and XeF laser irradiation to the base glass as typical examples. These results indicate that equation (4) produced the time evolution curves of the induced absorption well. In table 2, the parameters of the fitting curves for all the irradiation conditions are summarized.

More detailed models, e.g., involving intermediate reactants, as proposed by Natura *et al* [26], might produce theoretical curves which more precisely fit to the experimental ones. In the present analyses, however, we have relied on the simpler model because it could present the important features of the experimental results.

It is worth noting that the pulse intensity dependence of the number of generated NBOHCs after saturation was different between the ArF and XeF lasers. The number of NBOHCs, or the absorption intensities due to the defects, after saturation were independent of the pulse intensities for the ArF laser irradiation, while for the XeF laser irradiation the saturation value from high intensity pulses was higher than that from low intensity pulses.

The model proposed in the previous section can explain the different behavior. After a long irradiation time, $k_r t \rightarrow \infty$, the amount of the generated NBOHCs is expressed by

$$N = \frac{k_f}{k_r} N_0. \tag{5}$$

For irradiation at 193 nm with the ArF laser, a one-photon process is expected because the laser energy is higher than the energy of the absorption edge of the glass. Then, k_f is represented by

$$k_f = k^0_{\mathrm{ArF}} q^{\kappa}, \tag{6a}$$

where q is the dose rate, or number of incident photons per unit time, and $\kappa \sim 1$ for the one-photon process. k^0_{ArF} is the rate constant for the NBOHC generation reaction at a unit ArF laser dose rate. For the reverse reaction, k_r is written

by the summation of the one-photon process and the thermal activation process,

$$k_r = k_r^0 q^\eta + k_h, \tag{7}$$

where $k_r^0 q^\eta$ and k_h are the rate constants of the one-photon and thermal activation processes, respectively, and $\eta \sim 1$. k_r^0 is again the rate constant for the reverse reaction at a unit ArF laser dose rate. Since the irradiation was performed at room temperature, the thermal reaction can be negligibly small compared with the photo-reaction, i.e. $k_r^0 q^\eta \gg k_h$. Then equation (5) becomes

$$N = \frac{k_{\mathrm{ArF}}^0}{k_r^0} q^{\kappa-\eta} N_0. \tag{8a}$$

Furthermore, since κ–η is almost zero, the number of generated defects, N, eventually becomes independent of the radiation intensity. On the other hand, for the XeF laser irradiation, the energy of the photon is less than the energy of the absorption edge of the glass. Here, multi-photon processes should occur for the defect generation. This leads to

$$k_f = k_{\mathrm{XeF}}^0 q^\mu, \tag{6b}$$

where k_{XeF}^0 is the rate constant at a unit XeF laser dose rate and μ is larger than one. Since the two-photon energy is enough to excite an electron over the absorption edge, a two-photon process is assumed in the present analysis. Thus, $\mu \sim 2$, and

$$N = \frac{k_{\mathrm{XeF}}^0}{k_r^0} q^{\mu-\eta} N_0, \tag{8b}$$

where μ–$\eta \sim 1$, resulting in a dependence of N on the radiation intensity[6]. These predictions were very consistent with the experimental results, as shown in figure 5.

3.3.3. Laser intensity dependence. When $(k_r t)^\beta \to 0$, the number of generated NBOHCs, N, is approximately written by

$$N = \frac{k_f}{k_r} N_0 (k_r t)^\beta = k_f k_r^{\beta-1} N_0 t^\beta. \tag{9}$$

From equations (6) and (7), equation (9) becomes

$$N = k_{\mathrm{ArF}}^0 (k_r^0)^{\beta-1} q^{\kappa+(\beta-1)\eta} N_0 t^\beta \tag{10a}$$

$$N = k_{\mathrm{XeF}}^0 (k_r^0)^{\beta-1} q^{\mu+(\beta-1)\eta} N_0 t^\beta \tag{10b}$$

for the ArF and XeF laser, respectively. Here, $0 < \beta < 1$, as evaluated by the fittings (experimentally ~0.3 and 0.5–0.7 for the ArF and XeF lasers, respectively, as shown in table 1), then the exponential dependence of the N on the intensity of the ArF and XeF lasers are expected to be less than 1 and 2, respectively. This prediction is consistent with the experiments, as shown in figure 6.

[6] We also used equation (7) for the XeF laser irradiation. More strictly, the parameters, k_r^0 and η, might not be the same as those of the ArF laser irradiation. However, the dependence on the pulse intensity is probably the same because the absorption due to the NBOHC is in the visible region and the photon energy of the XeF laser is higher than it.

3.4. Effect of iron doping

Finally, we discuss the difference between the base and Fe-doped glasses. We have investigated defect generation behaviors in soda-lime silicate glasses doped with various amounts of Fe_2O_3 [38]. More NBOHCs were generated by the x-ray irradiation in soda-lime silicate glasses containing 0.01–0.07 wt% of Fe_2O_3 than that in base (undoped) glass, while the stability of the NBOHCs against recombination with electrons was highest for the base glass. We explain these experimental results by the fact that Fe^{3+} and Fe^{2+} ions play a role of electron- and hole-trapping sites, respectively. Such electron- and hole-trapping reactions by transition metals, stably existing as multivalent ions in glasses, have been also reported for other metals than iron. In the present study, the NBOHCs generated in the Fe-doped glass by the ArF laser irradiation were slightly fewer than those in the base glass. However, this might be not due to the role as the electron- and hole-trapping sites of the iron but due to the strong absorption in the ultraviolet region relevant to the iron ions. This absorption decreases the number of photons available for defect generation in the Fe-doped glass.

4. Conclusions

Irradiation with the excimer lasers, ArF at 193 nm, KrF at 248 nm, and XeF at 351 nm, of soda-lime silicate and Fe-doped soda-lime silicate glasses generated various kinds of defects, i.e., non-bridging oxygen hole centers, E′ centers, and electron-trapped centers, as occurs in the cases of x-ray and γ-ray irradiation. Glasses irradiated by the ArF laser were brownish colored, as detectable by naked eye observation. The formation behavior of the non-bridging oxygen hole centers was explained by a simple reaction model based on the reversible generation and annihilation of defects assuming one-photon (for ArF laser) and two-photon (for XeF laser) processes. The coloration due to the induced non-bridging oxygen hole centers will be used for laser drawing and marking of glasses.

Acknowledgment

This work was financially supported by the New Energy and Industrial Technology Development Organization (NEDO).

References

[1] Griscom D L 1978 *J. Non-Cryst. Solids* **31** 241
[2] Griscom D L 1984 *J. Non-Cryst. Solids* **64** 229
[3] Griscom D L 1985 *SPIE Proc.* **541** 38
[4] Maekawa T, Murai N, Haino K and Yokokawa T 1989 Nippon Seramikkusu Kyokai Gakujutsu Ronbunshi *J. Ceram. Soc. Japan* **97** 385
[5] Friebele E J 1991 Radiation effects *Optical Properties of Glasses* ed D R Uhlmann and N J Kreidl (Westerville, OH: The American Ceramic Society) p 205
[6] Imai H, Arai K, Hosono H, Abe Y, Arai T and Imagawa H 1991 *Phys. Rev.* B **44** 4812
[7] Imai H, Arai K, Isoya J, Hosono H, Abe Y and Imagawa H 1993 *Phys. Rev.* B **48** 3116

[8] Kadono K, Akai T, Yamashita M, Sheng J, Chen S, Yao Z, Itakura N, Yamane T, Utagawa Y, Matsumoto Y and Yazawa T 2002 *Proc. SPIE* **5061** 156
[9] Kadono K, Itakura N, Akai T, Yamashita M and Yazawa T 2009 *Nucl. Instrum. Methods Phys. Res.* B. **267** 2411
[10] Chen S, Akai T, Kadono K and Yazawa T 2001 *Chem. Commun.* 2090
[11] Chen S, Akai T, Kadono K and Yazawa T 2001 *Appl. Phys. Lett.* **79** 3687
[12] Sheng J, Kadono K, Utagawa Y and Yazawa T 2002 *Appl. Radiat. Isot.* **56** 621
[13] Yamashita M, Yao Z, Matsumoto Y, Utagawa Y, Kadono K and Yazawa T 2004 *J. Non-Cryst. Solids* **333** 37
[14] Kajihara K, Skuja L, Hirano M and Hosono H 2001 *Appl. Phys. Lett.* **79** 1757
[15] Hosono H, Ikuta Y, Kinishita T, Kajihara K and Hirano H 2001 *Phys. Rev. Lett.* **87** 175501
[16] Kajihara K, Ikuta Y, Hirano H and Hosono H 2002 *Appl. Phys. Lett.* **81** 3164
[17] Kajihara K, Skuja L, Hirano M and Hosono H 2002 *Phys. Rev. Lett.* **89** 135507
[18] Kajihara K, Ikuta Y, Hirano M and Hosono H 2003 *J. Non-Cryst. Solids* **322** 73
[19] Wang R P, Saito K and Ikushima A J 2005 *J. Non-Cryst. Solids* **351** 1569
[20] Kajihara K, Skuja L, Hirano M and Hosono H 2006 *Phys. Rev.* B **74** 094202
[21] Kajihara K 2007 *J. Ceram. Soc. Japan* **115** 85
[22] Natura U and Ehrt D 1999 *Glastech. Ber. Glass Sci. Technol.* **72** 295
[23] Ehrt D, Ebeling P and Natura U 2000 *J. Non-Cryst. Solids* **263/264** 240
[24] Natura U, Feurer T and Ehrt D 2000 *Nucl. Instrum. Methods Phys. Res.* B **166** 470
[25] Natura U and Ehrt D 2001 *Nucl. Instrum. Methods Phys. Res.* B **174** 143
[26] Natura U and Ehrt D 2001 *Nucl. Instrum. Methods Phys. Res.* B **174** 151
[27] Möncke D and Ehrt D 2004 *Glass Sci. Technol.* **77** 239
[28] Möncke D and Ehrt D 2006 *J. Non-Cryst. Solids* **352** 2631
[29] Montenero A, Friggeri M, Giori D C, Belkhiria N and Pye L D 1986 *J. Non-Cryst. Solids* **84** 45
[30] Ades C, Toganidis T and Traverse J P 1990 *J. Non-Cryst. Solids* **125** 272
[31] Bingham P A, Parker J M, Searle T, Williams J M and Fyles K 1999 *J. Non-Cryst. Solids* **253** 203
[32] Sigel G H Jr and Ginther R J 1968 *Glass Technol.* **9** 66
[33] Griscom D L, Gingerich M E and Friebele E J 1993 *Phys. Rev. Lett.* **71** 1019
[34] Mashkov V A, Austin W R, Zhang L and Leisure R G 1996 *Phys. Rev. Lett.* **76** 2926
[35] Griscom D L 2001 *Phys. Rev.* B **64** 174201
[36] Saito R and Murayama K 1987 *Solid State Commun.* **63** 625
[37] Crandall R S 1991 *Phys. Rev.* B **43** 4057
[38] Kadono K, Itakura N, Akai T, Yamashita M and Yazawa T 2009 *J. Non-Cryst. Solids* at press